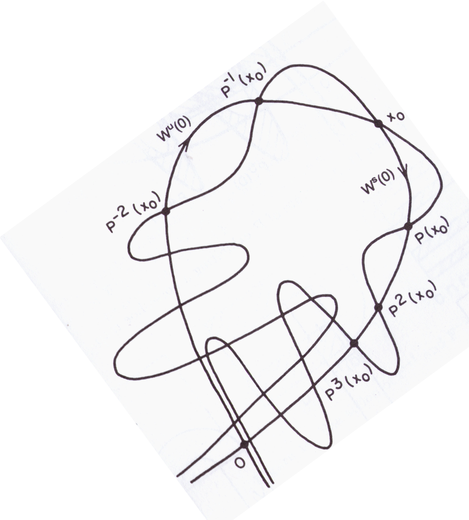

Hurricanes, Horseshoes, and Homoclinic Tangles

Visualizing Transport and Lobe Dynamics in Tropical Storms

Philip Du Toit, Jerrold Marsden
California Institute of Technology

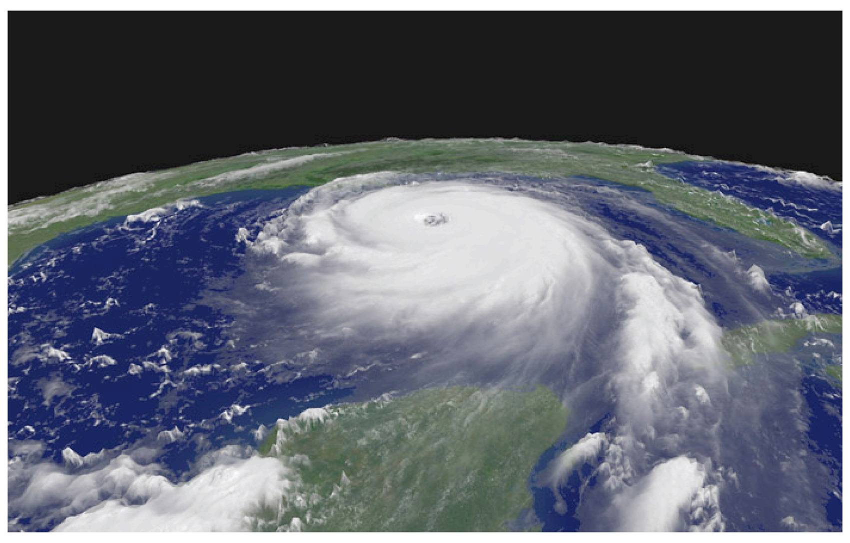

0. Extracting Transport Structures using Finite Time Liapunov Exponents

Figure 1: We are given a time-dependent vector field

$$\dot{\mathbf{x}} = \mathbf{v}(\mathbf{x}, t)$$

A trajectory is the solution of the initial value problem:

$$\begin{aligned} \dot{\mathbf{x}}(t; t_0, \mathbf{x}_0) &= \mathbf{v}(\mathbf{x}(t; t_0, \mathbf{x}_0), t) \\ \mathbf{x}(t_0; t_0, \mathbf{x}_0) &= \mathbf{x}_0. \end{aligned}$$

The flow map maps points forward in the flow.

Figure 2: Compute the Finite Time Liapunov Exponent (FTLE) using derivatives of the flow map.

$$\sigma_t^T(\mathbf{x}) := \frac{1}{|T|} \ln \left\| \frac{d\phi_t^{t+T}}{d\mathbf{x}} \right\|_2$$

Define the Lagrangian Coherent Structures (LCS) as ridges in the FTLE. This methodology follows that of Haller, Shadden, Lekien, Couillette, and Marsden.

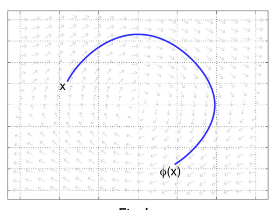

Fig 1

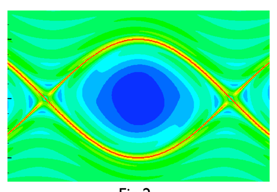

Fig 2

All computations of the FTLE were computed using codes developed recently at Caltech.

The code has the following features:

1. **N-dimensional**: The FTLE can be computed for flows in N dimensions for arbitrary N. Recent applications to transport in the phase space of the solar system have required 6 dimensional computations, for example.

2. **Parallel:** The code exploits independence of trajectory calculations to perform computations efficiently in parallel resulting in dramatic speed up.

3. **Modular**: The code is written in C++ language to facilitate modularity. Code additions and subtractions can be easily made.

4. **Efficient Data Structures:** The code is designed for analysis of large data sets. Light-weight data structures allow for efficient use of limited available memory.

5. **Features for Geophysical Applications:** The code allows for computation on the sphere, storm tracking for computation in storm-centered coordinates, using nested grid data, and non-uniformly spaced grids that are convenient for geophysical applications.

1. Lagrangian Coherent Structures and Lobe Dynamics in a Simple Model

Figure 3: The wind field at the 850mb pressure level obtained from NCAR-NCEP Reanalysis data. The vortex evident North East of Japan is Typhoon Nabi (2005).

Figures 4a-c: A simple kinematic model for typhoon flow is given by superimposing a periodically perturbed vortex in a background linear shear flow. The velocity field is:

$$\begin{aligned} u &= \frac{-(y - y_0)}{x^2 + (y - y_0)^2 + \alpha} - \beta \\ v &= \frac{x}{x^2 + (y - y_0)^2 + \alpha} + \epsilon\, y \cos 2t\,. \end{aligned}$$

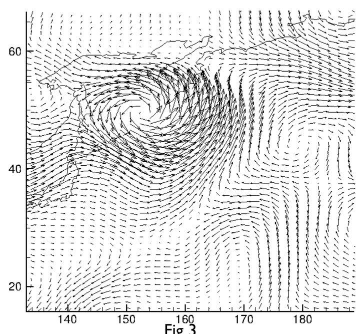

Fig 3

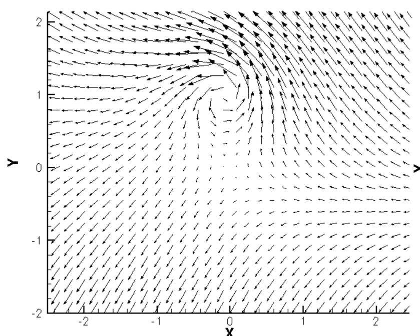

Fig 4a

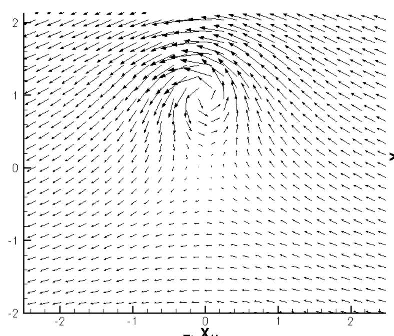

Fig 4b

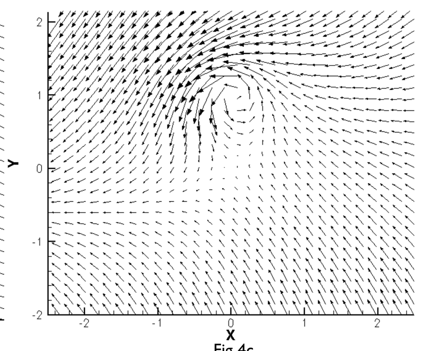

Fig 4c

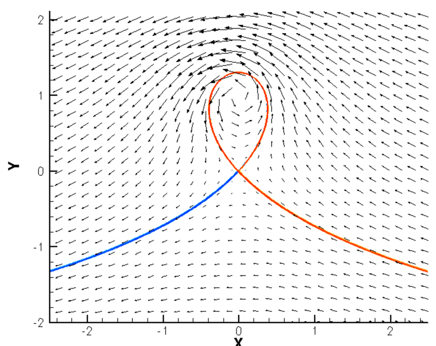

Fig 5

Figure 5: Superposition of the attracting (blue) and repelling (red) LCS computed for the unperturbed flow reveals the familiar homoclinic connection from geometric dynamics.

Figure 6: A snapshot of the LCS for the perturbed model vortex.

Figures 7a-d: A sequence illustrating how the LCS delineate the boundaries of lobes and reveal transport via lobe dynamics. Blue drifters are detrained while red drifters are entrained into the vortex.

Fig 6

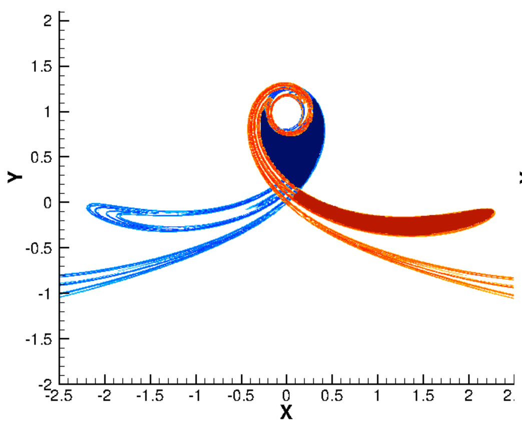

Fig 7a

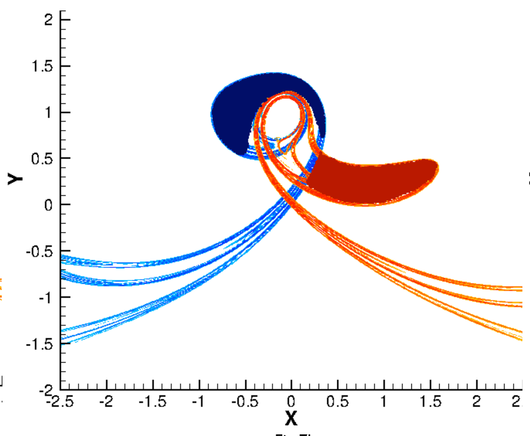

Fig 7b

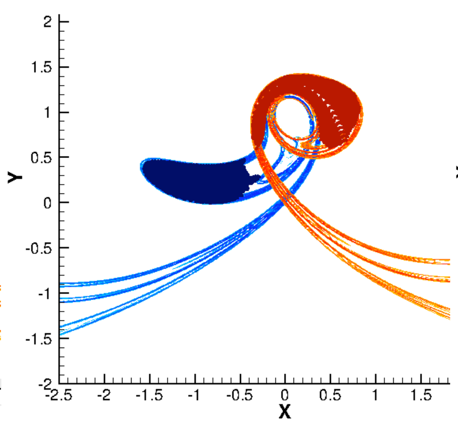

Fig 7c

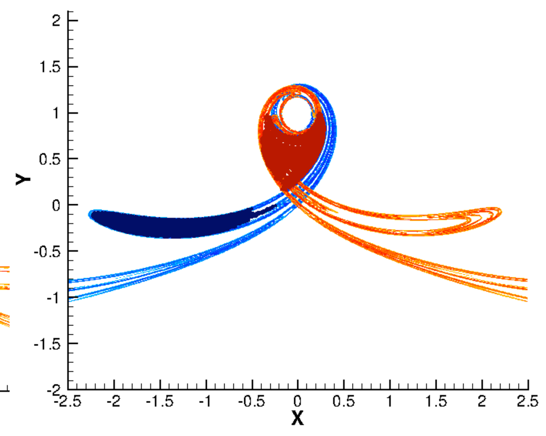

Fig 7d

2. Lobe Dynamics in the Large-Scale Flow of Typhoon Nabi

Figure 8: Computation of the attracting and repelling LCS for the windfield of Typhoon Nabi reveals a sharply-defined boundary for the vortex that cannot be determined by mere inspection of the velocity or vorticity fields.

Figure 9: Furthermore, intersections of the LCS define lobes colored brown and green that will be entrained and detrained via the action of lobe dynamics.

Figures 10a-c: Snapshots of the evolution of the LCS reveals how the green lobe is entrained into the vortex while the brown lobe is detrained via the action of lobe dynamics.

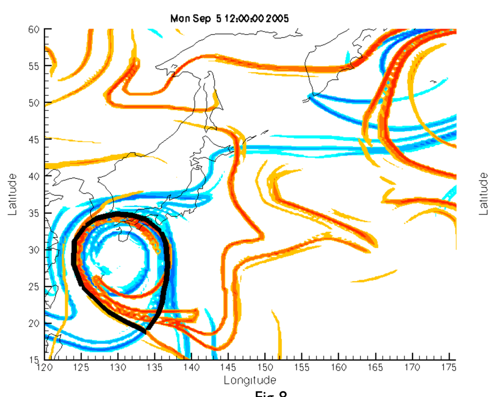

Fig 8

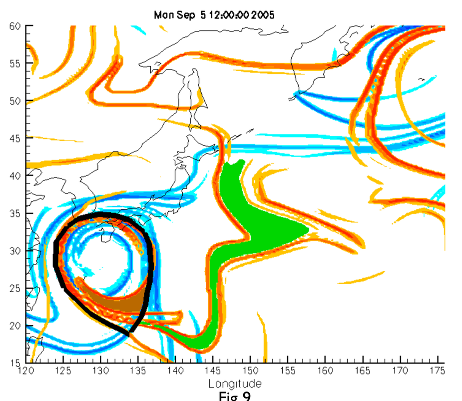

Fig 9

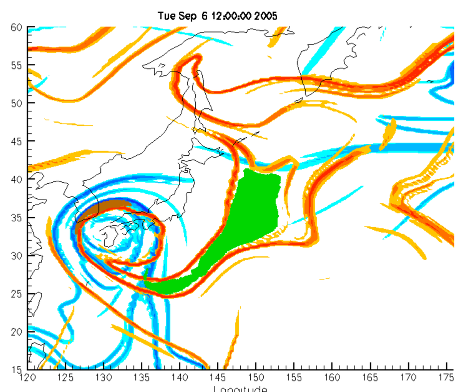

Fig 10a

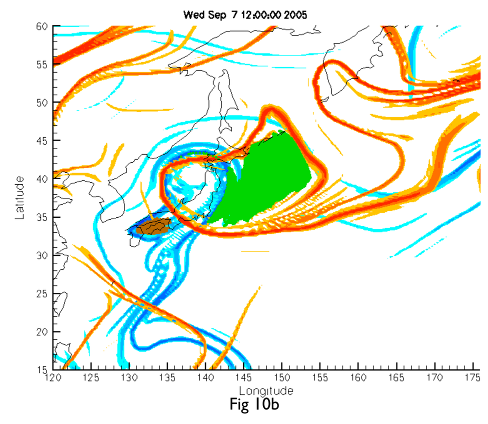

Fig 10b

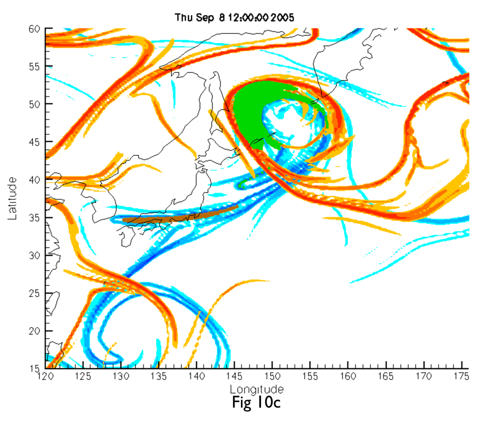

Fig 10c

Figure 11: A satellite image of Typhoon Nabi that struck Japan in September 2005.

Figure 12: A textbook illustration of the classical homoclinic tangle associated with a perturbed homoclinic connection.

Figure 13: The LCS captures the homoclinic tangle in the simple kinematic model.

Figures 14a-c: The LCS for several typhoons is compared with that of the simplified model and reveals that lobe dynamics is a dominant transport mechanism in tropical storms.

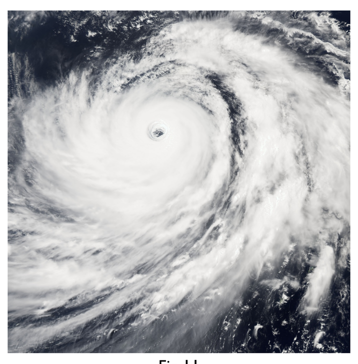

Fig 11

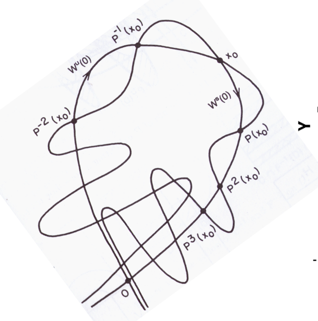

Fig 12

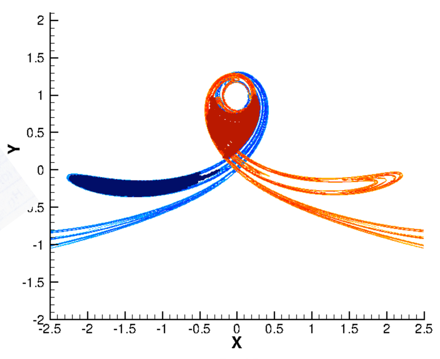

Fig 13

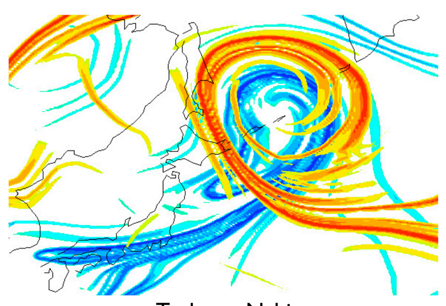

Typhoon Nabi

Fig 14a

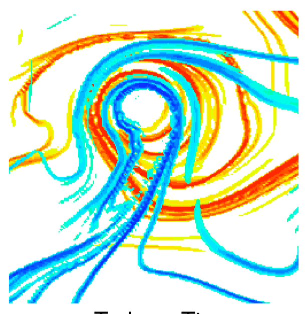

Typhoon Tip

Fig 14b

Typhoon Banyan

Fig 14c

3. Transport Structures near the Eyewall in Hurricane Isabel

Figure 15: Satellite image of Hurricane Isabel.

Figures 16a-c: High resolution models capture the process of eyewall replacement in which the eyewall disintegrates and is replaced by an eyewall of larger radius which subsequently contracts. The intensity of the storm fluctuates markedly during this process.

Figure 17: The New York Times carried an article explaining how meteorologists must accurately model the physics of eyewall replacement in order to improve predictions of hurricane intensity.

Fig 15

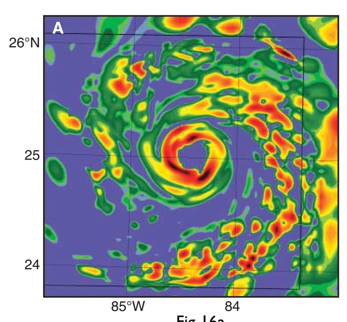

Fig 16a

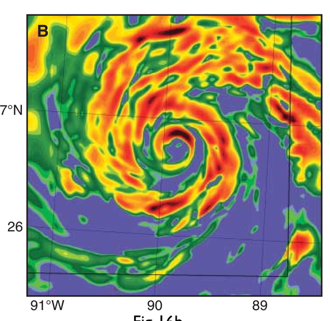

Fig 16b

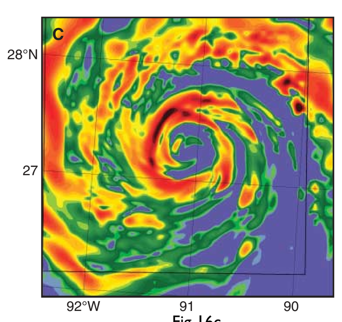

Fig 16c

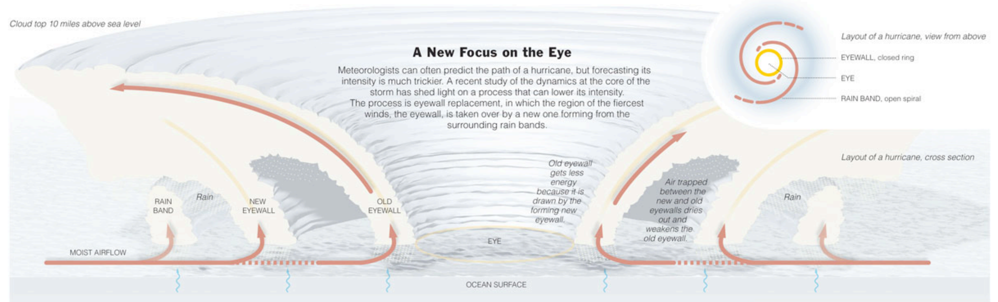

The New York Times Fig 17 29 May 2007

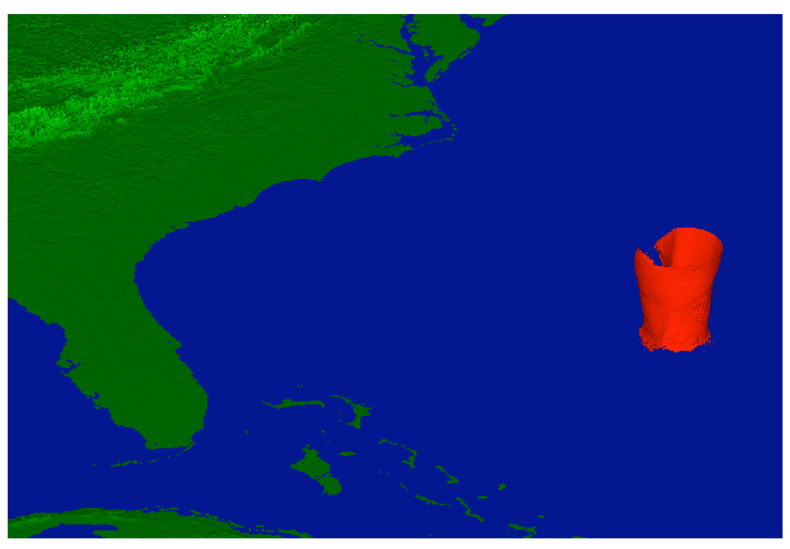

Fig 18

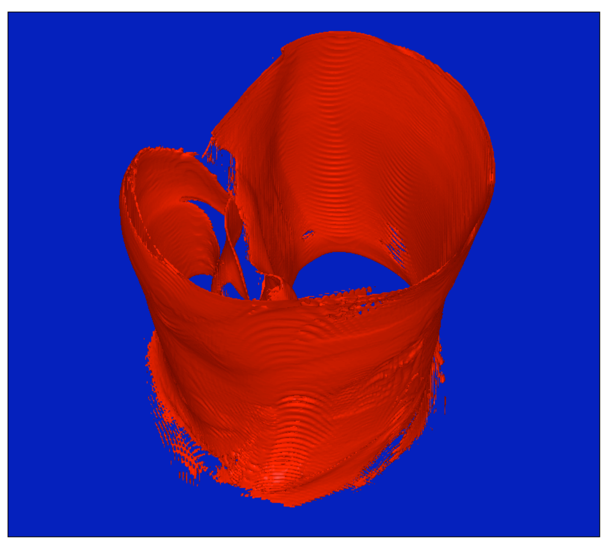

Fig 19a

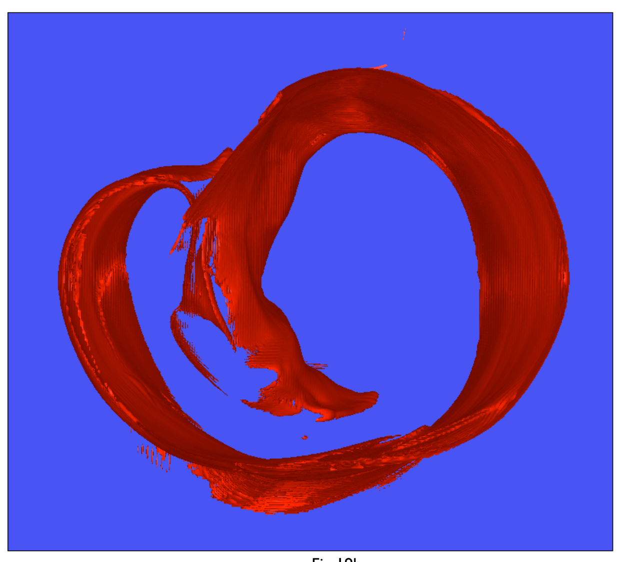

Fig 19b

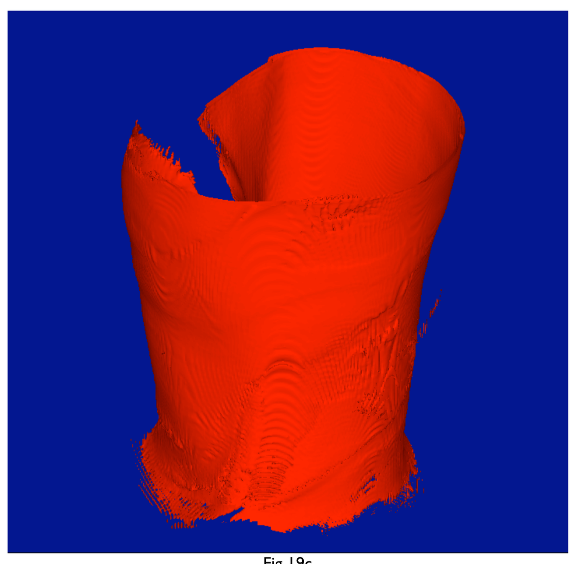

Fig 19c

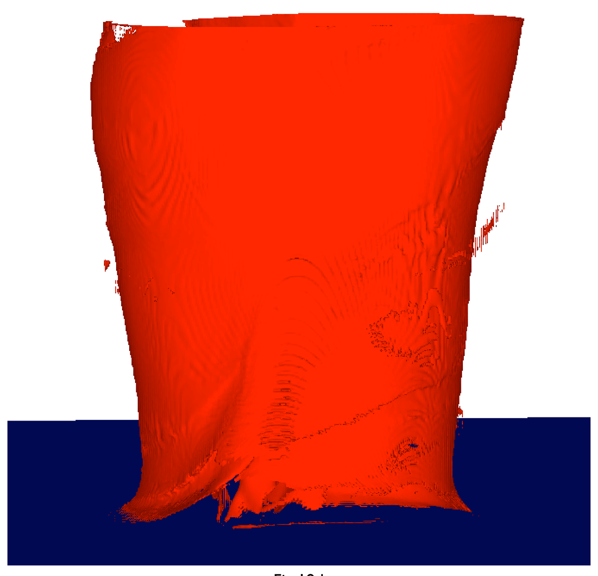

Fig 19d

Figures 18: The repelling LCS computed in 3D for Isabel reveals the Lagrangian eyewall structure.

Figures 19a-d: The eyewall structure is viewed from several angles. The eyewall computed with LCS uses Lagrangian dynamics of the flow and is not obtained using inspection of the Eulerian velocity field as is typically done in meteorology.

Figures 20a,b: The eyewall as determined by LCS is a dynamical barrier in the flow that separates regions of different dynamical behavior. To illustrate this, we place drifters colored red, green, and blue in different regions relative to the eyewall.

Figures 21a-d: A sequence of snapshots of the drifter trajectories in Hurricane Isabel show how the LCS separates regions of different dynamical behavior. The blue drifters are quickly advected into the upper atmosphere while the red drifters remain trapped in the eyewall. Interestingly, green drifters that initially start within a lobe protruding from eyewall, are eventually stripped off the eye and exit to the upper atmosphere. Further study will determine how these processes are related to eyewall replacement.

Figures 22a-d: The same sequence of snapshots of drifters in Hurricane Isabel is shown from above.

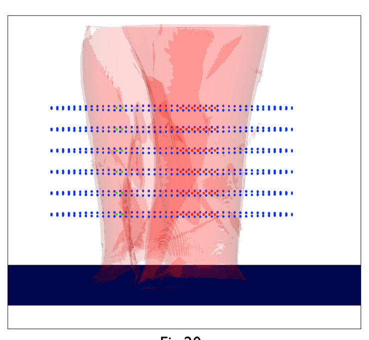

Fig 20a

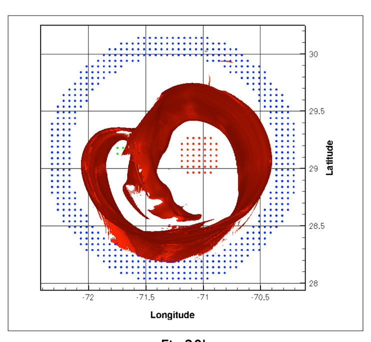

Fig 20b

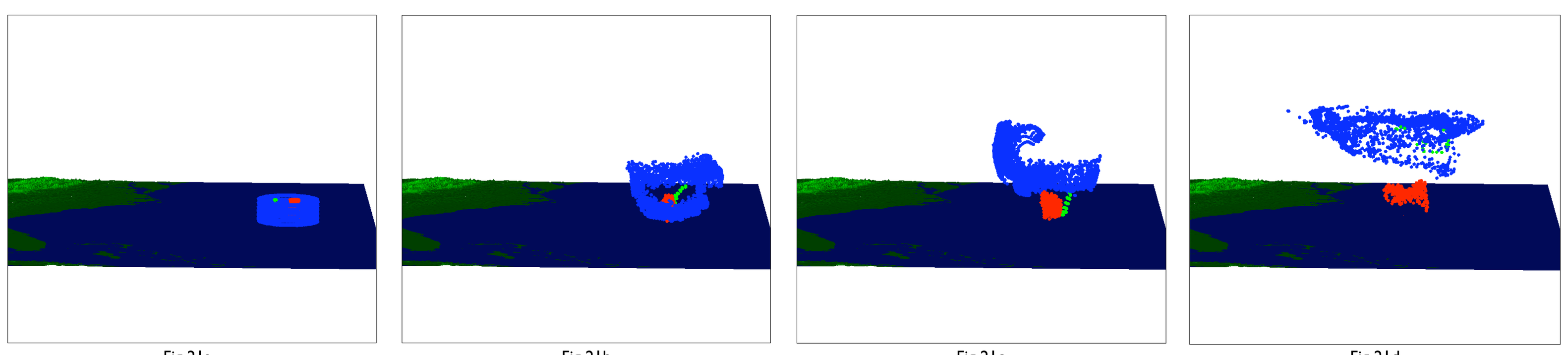

Fig 21a Fig 21b Fig 21c Fig 21d

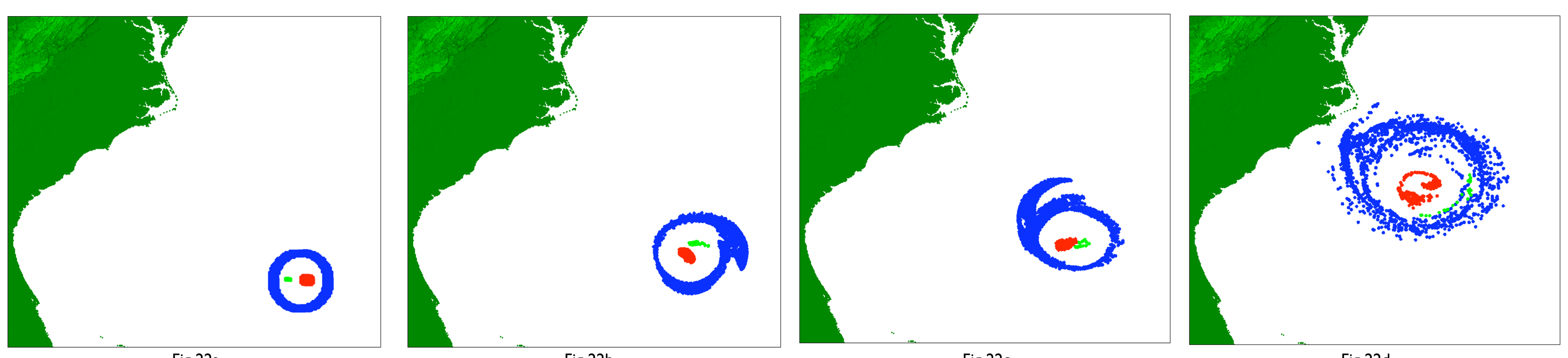

Fig 22a Fig 22b Fig 22c Fig 22d